Hypoxia-Related Immune Gene Signature Predicting Prognosis in Patients With Hepatocellular Carcinoma

Lingshan Zhou
Lanzhou University First Affiliated Hospital
Yuan Yang
Lanzhou University First Affiliated Hospital
Min Liu
Lanzhou University First Affiliated Hospital
Rong Liu
Lanzhou University First Affiliated Hospital
Man Ren
Lanzhou University First Affiliated Hospital
Ya Zheng
Lanzhou University First Affiliated Hospital
Yuping Wang
Lanzhou University First Affiliated Hospital
Yongning Zhou (yongningzhou@sina.com)
Lanzhou University First Affiliated Hospital

Research

Keywords: Hypoxia, immune, prognosis, Hepatocellular carcinoma

Posted Date: May 12th, 2021

DOI: https://doi.org/10.21203/rs.3.rs-476159/v1

Abstract

Background

Hepatocellular carcinoma (HCC) remains a global health challenge. Increasing evidence indicates that hypoxia is crucial in the evolution and progression of HCC by regulating the tumor immune microenvironment. The present study aimed to construct a prognostic relevant hypoxia-related immune gene (HRIG) signature.

Methods

We analyzed the expression profile of the 163 HRIGs and clinical information of 371 patients with HCC obtained from The Cancer Genome Atlas (TCGA). Then, consensus clustering analysis was performed to divide HCC patients into clusters 1 and 2 based on the HRIG expression. Subsequently, A multigene signature was constructed by Least absolute shrinkage and selection operator (LASSO) Cox regression analyses. Then, we evaluated the prognostic capability of this signature by Kaplan-Meier analysis, univariate Cox regression and multivariate Cox regression. The prognostic value of the signature was validated in the International Cancer Genome Consortium (ICGC) database. Furthermore, the functional enrichment analyses were preformed to elucidate their biological significance. Finally, we evaluated the infiltration of immune cells and the sensitivity of administrating chemotherapeutic agents.

Results

A total of 37 prognosis-related HRIGs were obtained. Subsequently, we constructed an 8-gene signature on the basis of prognosis-related HRIGs, which had a good performance in predicting the overall survival of patients with HCC. In addition, the signature expressed robust when validated in ICGC. The results revealed that these genes involved in some of the HCC-related pathways and was associated with the infiltration of immune cell subtypes. More importantly, the identified model was linked to the sensitivity of some chemotherapeutic agents.

Conclusions

HRIG signature is an effective predictor for the prognosis of patients with HCC.

Background

Primary liver cancer is the sixth most common cancer in the world and the third leading cause of cancer-related mortality, accounting for approximately 906,000 new cases and 830,000 deaths in 2020 [1]. Globally, hepatocellular carcinoma (HCC) is the most common form of primary liver cancer and comprises 75%-85% of cases, which pose a serious health burden [1, 2]. Many efforts have been made to develop surveillance systems and treatment strategies that include liver resection, radiofrequency ablation, liver transplantation, radiotherapy, systemic treatment and immunotherapy [3]. However, the prognosis of HCC remains poor (5-year survival rate of 5%) due to the high recurrence rate and the lack of diagnostic tools for early detection [4]. More than 75% of HCC patients are diagnosed at advanced stage and curative treatments are not recommended [5]. Furthermore, the recurrence of primary HCC is as high as 70% after clinical resection [6]. Hence, it is imperative to search for novel biomarkers for early detection, predicting the prognosis, and prediction and monitoring for treatment response of HCC.

Many solid tumors exist in an oxygen-starved environment due to the relative inadequate blood supply. Hypoxia occurs in about 50-60% of advanced solid tumors and the potential roles in the pathophysiological process of cancers have attracted lots of interest [7]. To adapt to the low oxygen conditions, the hypoxia inducible factor (HIF) stabilization and downstream signaling are induced, resulting in the numerous changes in gene expression [8]. The related molecular mechanisms of hypoxia play important roles in regulating cell proliferation and survival, induction of angiogenesis, driver of epithelial-to-mesenchymal (EMT), increasing therapeutic resistance and reprograming metabolism in cancer [9]. And hypoxia has become one attractive therapeutic target in cancer [10]. In recent years, more and more evidences emphasize the significant of hypoxia in the prognostic evaluation of cancers.

Hepatocarcinogenesis is a multistep process driven by liver inflammation and tissue damage. Liver damage disrupts the microvasculature and decreases of the blood flow, leading to the hypoxia situation [11]. Hypoxia microenvironment is common in HCC and has an intimate association with hepatocarcinogenesis, the progression and the recurrence of HCC [12, 13]. The key molecular mechanism induced by hypoxia is through the stabilization of transcription factor, hypoxia-inducible factors (HIFs) [14]. And HIF-1α and HIF-2α are highly expressed in HCC and significantly associated with poor prognosis of HCC 15. Many researches reveal that HIFs have an intimate link with tumor immunity. HIFs can act as central regulators to damage and inhibit the innate immune response of liver cancer, resulting in immune evasion and creation of immunosuppressive microenvironment [11]. Moreover, HIFs have effect on the adaptive immune system by transcriptionally activate their target genes that are important for the exhaustion of T cell, NK cell and M1 macrophages, and the enrichment of Treg and M2 macrophages [11, 16]. However, the relationship between hypoxia-related immune genes and the prognosis of HCC is still far from clear.

In this study, we analyzed the datasets of HCC patients from The Cancer Genome Atlas (TCGA) and identified the differentially expressed hypoxia-related immune genes (DEHRIGs) related to the overall survival (OS). Then, a prognostic model with DEHRIGs was constructed to predict the survival potential and validated in the ICGC cohort. We further explored the underlying mechanisms by performing functional enrichment analyses and evaluating the characteristics of tumor immune in the high- and low-risk groups. Last, we screened the candidate agents by exploring the sensitivity of chemotherapeutic agents. The flow diagram of the study was shown in Fig .1.

Methods

Data source

The RNA-seq transcriptome data and corresponding clinical data regarding 371 HCC were downloaded from the TCGA project (https://portal.gdc.cancer.gov). Molecular Signatures Database (MSigDB version 6.0) were performed to identify hypoxia-related genes (HRGs) http://software.broadinstitute.org/gsea/msigdb[17]. Finally, 199 HRGs were rolled in the analysis of the study. Similarly, 1811 immune-related genes were acquired from ImmPort database (http://www.immport.org). The ICGC dataset with another 231 HCC patients was used as a validation cohort to assess the prognostic potential of the risk score (https://dcc.icgc.org/projects/LIRI-JP).

Consensus clustering analysis based on hypoxia-related immune genes (HRIGs)

We assessed the correlation between HRGs and immune-related genes. And the hypoxia-related immune gene (HRIGs) were identified, according to the thresholds of correlation coefficients of > 0.4 and P-value of<0.001. In order to elucidate the biological function of HRIGs in HCC, we classified the HCC samples into different subtypes with the “ConsensusClusterPlus” (50 iterations and resample rate of 80%).

Construction and validation of a HRIG prognostic signature

The R package limma was performed to screen the differentially expressed HRIGs with the thresholds of adjusted false discovery rate (FDR) P-value of <0.05. Sequentially, the univariate Cox regression analysis of OS was performed to obtain prognosis-related HRIGs in HCC by the STRING database (https://string-db.org/). And the genes were identified as prognostic-associated genes with P-value of <0.05. Then, we performed the least absolute shrinkage and selection operator (LASSO) algorithm to filter these prognosis-related HRIGs most correlated with OS by the “glmnet” R package. Subsequently, these filtered genes were rolled in the LASSO regression analysis to construct a prognostic signature with penalty parameter (λ) determined by 10-round cross-validation. The risk score of HRIG signature for each patient was calculated: Risk score=$\Sigma^{n}_{i=1}$(expression level of gene x regression coefficient). HCC patients were divided into high- and low- risk groups according to the median risk score determined by using "survminer" R package. Furthermore, we used R package stats and Rtsne to explore the characteristics of different groups by PCA and t-SNE, respectively. Finally, “timeROC” R package was used to assess the predictive potential of the gene signature by measuring the area under the receiver operating characteristic curve (AUC-ROC) [18].

Functional enrichment analyses

Subsequently, we screened the differentially expressed genes (DEGs) between high-risk and low-risk groups with the thresholds of absolute fold change (log2) of >1.5 and FDR of <0.05. To explore the underlying mechanism, we conducted the Gene Ontology (GO) and Kyoto Encyclopedia of Genes and Genomes (KEGG) analyses by using the "clusterProfiler" R package [19].

Evaluation of tumor-infiltrating immune cells

single-sample gene set enrichment analysis (ssGSEA) was performed to uncover the characteristics of immune cell infiltration by R package gsva [20]. We calculated the status of immune cell infiltration and relevant immune-related pathways among the HCC samples.

Exploration of the sensitivity of chemotherapeutic agents

To evaluate the sensitivity of chemotherapeutic drugs, we used the “pRRophetic” package in R to measure the half-maximal inhibitory concentration (IC50) of HCC patients in the high- and low-risk groups by ridge regression [21]. Based on the AJCC guidelines, cisplatin, mitomycin.C, vinblastine and sorafenib were selected as candidate antitumor drugs. Finally, we compared the IC50 in different groups by Wilcoxon signed-rank test.

Results

Correlation of consensus clustering for HRIGs with OS of HCC patients

We conducted Pearson correlation coefficient analysis to identify HRIGs. A total 163 HRIGs were screened and rolled in the subsequent differentialexpressionanalysis. Sequentially, consensus clustering analysis was performed based on the HRIG expression profiles. Based on the results with K=2 to 9, K=2 was identified as the optimal clustering value, which expressed the good clustering stability (Fig.S1a-b). Patients with HCC from TCGA cohort were dived into two molecular subgroups (cluster 1 and 2) (Fig.S1c). As shown in the Fig.1, cluster 1 exhibited more favorable prognosis than cluster 2. The results revealed that clustering cancer subtypes charactered by the HRIG expression were involve in the heterogeneity of HCC.

Analysis of differentially expressed HRIGs in HCC and identification of prognostic DE HRIGs in TCGA cohort

Among HRIGs, 89 DEHRIGs were identified (Fig.2a-b). Based on the survival data of HCC tumor samples, univariate Cox regression was conducted to identify the prognosis-related DEHRIGs. The results indicated that 37 DEHRIGs were correlated to OS in HCC. GHR, COLEC10 and VIPR1 were downregulated in tumor samples, while others were upregulated (Fig.2c-d). The result of the 37-gene interaction network generated by the STRING database showed that SRC, HSP90AB1, and SHC1 were Hub genes (Fig.2e). The correlation network of these genes was presented in Fig.2f.

Construction and validation of a HRIG prognostic signature

By LASSO Cox regression analysis, we built an 8-HRIG prognostic signature from the above 37 OS-related DEHRIGs. The risk score of every patient was computed based on the following formula. Risk score= 0.017176 × S100A10 + 0.226828 × MAPT + 0.021352 × CACYBP + 0.139515 × BIRC5 + 0.064381 × KITLG + 0.043464 × SPP1+ 0.145751 × STC2 + (-0.02423) × GHR. Based on the median risk score, 365 patients with HCC (after excluding 7 patients without time of follow-up) were divided into high-risk group (N=182) and low-risk group (N=183) (Fig.3a-b). PCA and t-SNE analyses indicated the patients were

distributed in two directions on the basis of risk score (Fig.3c-d). The Kaplan–Meier survival analysis showed that the patients in the high-risk group exhibited significant shorter OS compared with those in the low-risk group (Fig.3e). The AUC-ROC of the prognostic signature calculated from TCGA was 0.787 at 1 year, 0.724 at 3 years, 0.688 at 5 years, indicating the HRIG prognostic signature had a good performance in monitoring survival (Fig.3f). To verified the robustness of the HRIG prognostic signature, we evaluated the predictive value of the identified HRIG signature in the ICGC dataset. The risk score of every patient with HCC was calculate based the above formula and the patients were also categorized into high-risk and low-risk groups by the median value (Fig.4a-b). Similar to the results above, patients in two subgroups from the ICGC cohort were also distributed in two directions (Fig.4c-d). As shown in Fig.4e, the patients in the high-risk group had a shorter survival time compared with those in the low-risk group, which was consistent with the result from the TCGA dataset. Besides, The AUC-ROC of the prognostic signature calculated from ICGC was 0.740 at 1 year, 0.758 at 3 years, 0.752 at 5 years (Fig.4f).

Independent prognosis analyses

We subsequently performed the univariate Cox regression analysis and univariate Cox regression analysis to identify independent prognostic factors for OS. Eventually, stage ($p < 0.001$, HR = 2.500, 95% CI [1.721–3.632]) and risk score ($p < 0.001$, HR = 4.711, 95% CI [3.009–7.374]) showed significant correlation with OS both in TCGA cohort and ICGC cohort (Fig.5a-b). After correction for other confounding factors, stage ($p < 0.001$, HR = 2.065, 95% CI [1.412–3.021]) and risk score ($p < 0.001$, HR = 4.394, 95% CI [2.736–7.059]) were still related to OS by univariate Cox regression analysis (Fig.5c-d), which proved that risk score and stage were both independent prognostic factors in patients with HCC.

Review and comparison of recent immune-related gene prognostic signatures constructed for HCC

To evaluated the predictive performance and application value of our signature, we further reviewed four recently published prognostic signatures associated with immune-related genes and compared them with this study. Notably, as shown in Table.1, our signature exhibited its superiority. Firstly, it was built by the hypoxia-related immune genes. Compared with other prognostic signatures with single immune genes, it was better able to reveal the complex interaction of various parameters of tumor microenvironment affecting the development and progress of HCC. Additionally, our signature exhibited better performance in predicting OS than the signature built by Pan et al [22]. Compared with other three signatures [23-25], HRIG signature expressed more robust when validated in anther cohort. Thus, the study provided a more precise predictor for the prognosis of HCC patients and could provide support in clinical decision-making.

Functional analyses and evaluation of Tumor Immune Infiltration

Pathways in KEGG and biological processes in GO were performed to further explore the potential influence of the classifier based on the risk score in HCC. The analyses indicated that differentially expressed genes between high- and low- risk groups were mainly enriched in immune-related signaling pathways, cancer-related pathways, metabolism-related pathways. (Fig.6a, c), which were validated in the ICGC cohort (Fig.6b, d).

To further explore the influence of risk score on the tumor immune microenvironment, we evaluated immune infiltration status in HCC samples. In both cohorts, the infiltration of aDCs, DCs, Macrophages, Th2_cells and Treg were significantly increased in the high-risk group ($P < 0.05$), suggesting great significance of these infiltrating immune cells in the progression of HCC. At the same time, the infiltration of NK cells was significantly decreased ($P < 0.05$) (Fig.7a-b). Subsequently, we investigated the potential correlation between the risk score and immune function. The score of Check-point, HLA and T_cell_co-stimulation were higher in the high-risk group, while the score of type_I_IFN_Reponse and type_II_IFN_Reponse were the opposite (Fig.7c-d).

Exploration of correlation between the risk model and the efficacy of chemotherapeutic agents

To evaluate the clinical value of the identified risk model, we investigated the relationship between risk score and the sensitivity of common administrating chemotherapeutics. The present study demonstrated that the higher risk score was linked to higher chemosensitivity in mitomycin.c and cisplatin, and lower chemosensitivity in vinblastine, respectively (Fig.8a-c). However, there is no connection between the risk score and chemosensitivity in sorafenib (Fig.8d). Thus, these results suggested that the model had potential predictive performance for chemosensitivity.

Discussion

Liver cancer is an extraordinarily heterogeneous malignant tumor, which is one of main obstacles to the implementation of precision medicine [26]. Although the histopathological classification of liver cancer has been modified and refined, it still cannot solve the problem that predict patient prognosis or response to therapy accurately [27]. With the development of high throughput sequencing technology, more and more genes with oncogenic functions or tumor suppressive functions were identified. The expression patterns of these genes are recurrently altered in HCC, which give tumor cells corresponding abilities to influence malignant behaviors, such as recurrence, metastasis and drug resistance, leading to different clinical outcomes [28]. One of most important objectives of precision medicine is to provide each cancer patient with most accurate and effective treatment based on the genomic characteristics of the cancer [29]. Without doubt, accurate prognostic biomarkers need to be identified for executing precision medicine in a personalized manner. The heterogeneity of tumor exists not only in the genotypes but also in the tumor microenvironment. The accumulation of genomic alterations may result in changes of microenvironment of liver cancer [27]. Immune cells and tissue hypoxia, the elements of tumor microenvironment, have been verified to play an important role in the development of HCC and treatment response [30]. In this study, therefore, we focus on the effect of tumor immunity and hypoxia on the prognosis of HCC, which is convincingly beneficial to understanding the mechanism of tumorigenesis and tumor development, and the improvement of personalized therapeutic approaches. Using the RNA-seq transcriptome data and corresponding clinical data of HCC obtained from the TCGA dataset, we constructed the 8-hypoxia-related immune gene prognostic signature. The 8-gene signature exhibited a good performance to predict OS of HCC in the training set and expressed robust when validated in another cohort.

Our prognostic signature contained eight genes (S100A10, MAPT, CACYBP, BIRC5, KITLG, SPP1, STC2, GHR). These genes were correlated with OS of HCC separately and showed a better performance when combined, for one reason that gene signature analysis can reflect the complex interaction of various genes

affecting hypoxia-related tumor immunity in cancer. S100A10, a member of S100 family, mediates the process of transforming plasminogen to an active protease and has been reported to link to the HCC tumorigenesis and progression [31]. As a binding partner of S100 family proteins, CACYBP was highly expressed in HCC, which was significantly associated with elevated AFP level, increased dead and recurrence events, and reduced OS [32]. BIRC5, also known as survivin, is the most potent member of the inhibitor of apoptosis protein (IAP) family and a vital promoter of development and progression of HCC. The overexpression of survivin affects the prognosis of patients with HCC by promoting cell proliferation, inhibiting cell apoptosis and inducing tumor stromal angiogenesis [33]. The osteopontin protein is encoded by the SPP1 gene. Osteopontin overexpression increases proliferation, stem-like properties, glycolysis, and resistance to chemotherapy of HCC cells, which correlates with poor prognosis of HCC patients [34]. Importantly, osteopontin can associate with HIF-1α to promote tumorigenesis [34]. In addition, it plays a critical role in the formation of immunosuppressive microenvironment of HCC [35]. Likewise, STC2 is a proliferation-facilitating gene and correlates with occurrence, development, and prognosis of HCC [36]. Summarily, these genes above have been verified to be associated with the poor prognosis of HCC, which was consistent with the result of our study. Moreover, in this model, GHR was positively correlated with OS of the patients with HCC. One study demonstrated that HCC patients with a significant down-regulation of GHR expression showed higher incidence of recurrence and poor survival rates [37], which also supported our results. Among these genes, MAPT had the highest coefficient and was considered to be the main contributing gene. Many researches have demonstrated that MAPT was correlated with the prognosis of many cancers. The controversial roles of MAPT in both oncogenesis and tumor suppression were reported in these cancers, depending on the cell type and context. In addition, MAPT is also involved in resistance to paclitaxel, platinum, and bicalutamide, which contributed to the poor prognosis [38, 39]. Several lines of evidence have also demonstrated the effect of KITLG in tumorigenesis [40]. However, the biological functions of MAPT and KITLG in HCC have not been elucidated and need further research. Thus it can be seen that the gene signature was closely related to the malignant behaviors of HCC and could be an accurate predictor.

As previously mentioned, multiple pathways were significantly enriched in the high-risk group, including ECM-receptor interaction pathway. The signature contained two ECM-related genes, S100A10 and SPP1 [35, 41]. As one of the critical components in the tumor microenvironment, dysregulated ECM has been involved in the development and progression of HCC [42]. Hypoxia is one of the key inducers of the dysregulated ECM, by affecting ECM deposition, remodeling and degradation [43]. As shown in our analyses, HCC samples in the high-risk group had higher proportions of macrophages. Interestingly, Hypoxia can recruitment macrophages and induce the alteration of macrophages toward protumor phenotype in the tumor microenvironment, which contribute to ECM remodeling in favor of tumorigenesis and cancer progression [43, 44]. At the same time, ECM stiffness through induction of hypoxia is also a barrier for delivery of chemotherapeutic drugs to the tumor site, which weakens the efficacy of antitumor drugs [44]. The high resistance to antitumor drugs is one of the main contributors to the poor outcome of patients with advanced HCC who have no opportunity for surgical resection. The eight genes included in the signature are all linked to the drug resistance. Additionally, in the study, the patients in the high-risk group expressed the lower sensitivity to vinblastine. Apart from the mechanism mentioned above, hypoxia also contributes to the drug resistance by regulating the glycolytic metabolism. As a master regulator of glycolytic metabolism, HIF-1α activation can enhance the glycolytic metabolism at the transcriptional level, which influences the drug sensitivity in HCC [45]. The glycometabolism-related pathways were enriched in the high-risk group in the study. And glycolytic metabolism also takes roles for the regulation of proliferation, immune evasion, invasion, metastasis, angiogenesis in the liver cancer [46]. More importantly, metabolites released from cancer cells have an impact on the function of immune system cells, such as tumor-associated macrophages, NK cells, dendritic cells (DCs), regulatory T cells (Tregs) and cytotoxic T lymphocytes, leading to inhibition of the immune response [47, 48]. Notably, in addition to predicting the OS, the present results suggest that the eight-gene signature has a good performance in predicting the response of HCC patients to antitumor drugs. Therefore, the identified signature is a practical tool to help making clinical decision.

In addition to the above-mentioned macrophages, high-risk patients had significantly higher proportions of Tregs. Tregs belong in one category of tumour-infiltrating lymphocytes and play an important role in immune suppression [49]. Hypoxia has been identified in promoting the recruitment of Tregs to the tumour microenvironment by inducing the expression of CCL28, leading to promote tumour tolerance and angiogenesis [50]. In addition, these cells can suppress the functions of T cells, NK cells and DC [49]. As shown in the results, the score of type_II_IFN_Reponse was significantly lower in the high-risk group. T cell stimulation under hypoxia conditions inhibits the IFN-γ production [51]. In general, Hypoxia participates in accentuating the immunosuppressive characteristics of immune cells in the tumor environment of HCC, which may have important clinical significance for cancer immunotherapy and predicting the prognosis.

To our knowledge, this was the first study constructing a prognostic signature based on the hypoxia-related immune genes in HCC. Compared with the models based on the genes with single property, the signature contained higher information context. Additionally, the robustness and high predictive value strictly guaranteed the applicability of the signature. However, there were still some limitations in this study. We did the research by utilizing published retrospective data sets. Therefore, our findings should be validated in prospective studies. Furthermore, some important immune genes with prognostic potential were excludes in this research only based on hypoxia-related immune genes.

Conclusions

We identified the hypoxia-related immune genes and constructed an 8-gene prognostic signature through integrated analyses. The present results demonstrated that the HRIG signature was a reliable predictive marker for OS and response to the antitumor drugs in patients with HCC. Thus, the 8-gene signature might be a practical tool for facilitating personalized medicine and improving survival of HCC.

Abbreviations

HCC: Hepatocellular carcinoma; HRIG: Hypoxia-related immune gene; TCGA: The Cancer Genome Atlas; LASSO: Least absolute shrinkage and selection operator; ICGC: International Cancer Genome Consortium; HIF: Hypoxia inducible factor; DEHRIGs: Differentially expressed hypoxia-related immune genes; OS: Overall survival; HRGs: Hypoxia-related genes; AUC-ROC : Receiver operating characteristic curve; DEGs: Differentially expressed genes; GO: Gene Ontology; KEGG: Kyoto Encyclopedia of Genes and Genomes; ssGSEA: single-sample gene set enrichment analysis; IC50: half-maximal inhibitory concentration.

Declarations

Ethics approval and consent to participate

Not applicable.

Consent for publication

Not applicable.

Availability of data and materials

The data of this study are available in the TCGA and ICGC.

Competing interests

No conflicts of interest exist in this work.

Funding

This work was supported by the National Natural Science Foundation of China [grant number 81960430] and Hospital fund project of the first hospital of Lanzhou university [grant number ldyyyn2018-38].

Authors' contributions

Yongning Zhou supervised the project. Lingshan Zhou, Yuan Yang and Min Liu designed the workflow and performed the bioinformatic analysis. Yuling Gan, Rong Liu, Man Ren and Ya Zheng performed material preparation and data collection. Lingshan Zhou, Yuan Yang and Min Liu wrote the first draft. All authors commented on the manuscript. All authors read and approved the final manuscript.

Acknowledgements

Not applicable.

References

1. Sung H, Orcid Id, Ferlay J, et al. Global cancer statistics 2020: GLOBOCAN estimates of incidence and mortality. CA Cancer J Clin. 2021. ahead of print.
2. Petrick JL, X. Id- Orcid, Florio AA, et al. International trends in hepatocellular carcinoma incidence, 1978-2012. Int J Cancer. 2020;147(2):317-330.
3. Sun JY, Yin T, Zhang XY, et al. Therapeutic advances for patients with intermediate hepatocellular carcinoma. J Cell Physiol. 2019;234(8):12116-12121.
4. Trevisan França de Lima L, Broszczak D, Zhang X, et al. The use of minimally invasive biomarkers for the diagnosis and prognosis of. - Biochim Biophys Acta Rev Cancer. 2020;1874(2):188451.
5. Costentin C. Hepatocellular carcinoma surveillance. Presse Med. 2017 Apr;46(4):381-385.
6. Kulik L, Heimbach JK, Zaiem F, et al. Therapies for patients with hepatocellular carcinoma awaiting liver transplantation. Hepatology. 2018;67(1):381-400.
7. Tan Z, Xu J, Zhang B, et al. Hypoxia: a barricade to conquer the pancreatic cancer. Cell Mol Life Sci. 2020;77(16):3077-3083.
8. Xiong Q, Liu B, Ding M, et al. Hypoxia and cancer related pathology. Cancer Lett. 2020;486:1-7.
9. Hapke RY, Haake SM. Hypoxia-induced epithelial to mesenchymal transition in cancer. - Cancer Lett. 2020;487:10-20.
10. Jing X, Yang F, Shao C, et al. Role of hypoxia in cancer therapy by regulating the tumor microenvironment. Mol Cancer. 2019;18(1):157.
11. Yuen VW, Wong CC. Hypoxia-inducible factors and innate immunity in liver cancer. J Clin Invest. 2020;130(10):5052-5062.
12. Cui CP, Wong CC, Kai AK, et al. SENP1 promotes hypoxia-induced cancer stemness by HIF-1α deSUMOylation and. Gut. 2017;66(12):2149-2159.
13. Wu FQ, Fang T, Yu LX, et al. ADRB2 signaling promotes HCC progression and sorafenib resistance by inhibiting. J Hepatol. 2016;65(2):314-24.
14. Chen C, Lou T. Hypoxia inducible factors in hepatocellular carcinoma. Oncotarget. 2017;8(28):46691-46703.
15. Wong CC, Kai AK, Ng IO. The impact of hypoxia in hepatocellular carcinoma metastasis. Front Med. 2014 ;8(1):33-41.
16. Multhoff G, Vaupel P. Hypoxia Compromises Anti-Cancer Immune Responses. Adv Exp Med Biol. 2020;1232:131-143.
17. Liberzon A, Birger C, Thorvaldsdóttir H, et al. The Molecular Signatures Database (MSigDB) hallmark gene set collection. Cell Syst. 2015;1(6):417-425.
18. Blanche P, Dartigues JF, Jacqmin-Gadda H. Estimating and comparing time -dependent areas under receiver operating. Stat Med. 2013;32(30):5381-97.
19. Yu G, Wang LG, Han Y, et al. clusterProfiler: an R package for comparing biological themes among gene clusters. OMICS. 2012;16(5):284-7.
20. Hänzelmann S, Castelo R, Guinney J. GSVA: gene set variation analysis for microarray and RNA-seq data. BMC Bioinformatics. 2013;14:7.
21. Geeleher P, Cox NJ, Huang RS. Clinical drug response can be predicted using baseline gene expression levels and in. Genome Biol. 2014;15(3):R47.
22. Pan B, Orcid Id, Liu L, et al. A prognostic risk model based on immune-related genes predicts overall survival of. Health Sci Rep. 2020;3(4):e202.
23. Gu X, Guan J, Xu J, et al. Model based on five tumour immune microenvironment-related genes for predicting. J Transl Med. 2021;19(1):26.
24. Zhang J, Chen G, Zhang J, et al. Construction of a prognostic model based on nine immune-related genes and. Am J Transl Res. 2020;12(9):5108-5130.

25. Xu D, Wang Y, Zhou K, et al. Development and Validation of a Novel 8 Immune Gene Prognostic Signature Based on. Onco Targets Ther. 2020;13:8125-8140.
26. Zhang Q, Lou Y, Yang J, et al. Integrated multiomic analysis reveals comprehensive tumour heterogeneity and novel. Gut. 2019;68(11):2019-2031.
27. Li L, Wang H. Heterogeneity of liver cancer and personalized therapy. Cancer Lett. 2016;379(2):191-7.
28. Schulze K, Nault JC, Villanueva A. Genetic profiling of hepatocellular carcinoma using next-generation sequencing. J Hepatol. 2016;65(5):1031-1042.
29. Shin SH, Bode AM, Dong Z. Precision medicine: the foundation of future cancer therapeutics. NPJ Precis Oncol. 2017;1(1):12.
30. Tu T, Budzinska MA, Maczurek AE, et al. Novel aspects of the liver microenvironment in hepatocellular carcinoma pathogenesis. Int J Mol Sci. 2014;15(6):9422-58.
31. Zhao JT, Chi BJ, Sun Y, et al. LINC00174 is an oncogenic lncRNA of hepatocellular carcinoma and regulates. Cell Biochem Funct. 2020;38(7):859-869.
32. Lian YF, Huang YL, Zhang YJ, et al. CACYBP Enhances Cytoplasmic Retention of P27(Kip1) to Promote Hepatocellular. Theranostics. 2019;9(26):8392-8408.
33. Su C. Survivin in survival of hepatocellular carcinoma. Cancer Lett. 2016;379(2):184-90.
34. Song Z, Orcid Id, Chen W, et al. Osteopontin takes center stage in chronic liver disease. Hepatology. 2020. ahead of print.
35. Zhu Y, Orcid Id, Yang J, et al. Disruption of tumour-associated macrophage trafficking by the osteopontin-induced. Gut. 2019;68(9):1653-1666.
36. Wang Y, Wu J, Orcid Id, et al. Clinical significance of high expression of stanniocalcin-2 in hepatocellular. Biosci Rep. 2019;39(4):BSR20182057.
37. Lin CC, Liu TW, Yeh ML, et al. Significant down-regulation of GHR expression as a new unfavorable prognostic factor. Clin Mol Hepatol. 2020. ahead of print.
38. Sekino Y, Han X, Babasaki T, et al. Microtubule-associated protein tau (MAPT) promotes bicalutamide resistance and is. Urol Oncol. 2020;38(10):795.e1-795.e8.
39. Smoter M, Bodnar L, Grala B, et al. Tau protein as a potential predictive marker in epithelial ovarian cancer patients. J Exp Clin Cancer Res. 2013;32(1):25.
40. Yang Z, Orcid Id, Liu S, et al. High expression of KITLG is a new hallmark activating the MAPK pathway in type A and. Thorac Cancer. 2020;11(7):1944-1954.
41. Arai K, Ishimatsu H, Iwasaki T, et al. Membranous S100A10 involvement in the tumor budding of colorectal cancer during. World J Surg Oncol. 2020;18(1):289.
42. Mazza G, Telese A, Al-Akkad W, et al. Cirrhotic Human Liver Extracellular Matrix 3D Scaffolds Promote Smad-Dependent. Cells. 2019;9(1):83.
43. Gilkes DM, Semenza GL, Wirtz D. Hypoxia and the extracellular matrix: drivers of tumour metastasis. Nat Rev Cancer. 2014;14(6):430-9.
44. Najafi M, Farhood B, Mortezaee K, et al. Extracellular matrix (ECM) stiffness and degradation as cancer drivers. J Cell Biochem. 2019;120(3):2782-2790.
45. Bhattacharya B, Mohd Omar MF, Soong R. The Warburg effect and drug resistance. Br J Pharmacol. 2016;173(6):970-9.
46. Feng J, Li J, Wu L, et al. Emerging roles and the regulation of aerobic glycolysis in hepatocellular carcinoma. J Exp Clin Cancer Res. 2020;39(1):126.
47. Mossenta M, Busato D, Dal Bo M, et al. Glucose Metabolism and Oxidative Stress in Hepatocellular Carcinoma: Role and. Cancers (Basel). 2020;12(6):1668.
48. Icard P, Shulman S, Farhat D, et al. How the Warburg effect supports aggressiveness and drug resistance of cancer cells? Drug Resist Updat. 2018;38:1-11.
49. Kumar V, Gabrilovich DI. Hypoxia-inducible factors in regulation of immune responses in tumour. - Immunology. 2014;143(4):512-9.
50. Facciabene A, Peng X, Hagemann IS, et al. Tumour hypoxia promotes tolerance and angiogenesis via CCL28 and T(reg) cells. Nature. 2011;475(7355):226-30.
51. Westendorf AM, Skibbe K, Adamczyk A, et al. Hypoxia Enhances Immunosuppression by Inhibiting CD4+ Effector T Cell Function and. Cell Physiol Biochem. 2017;41(4):1271-1284.

Tables

Table 1 Review of recent immune-related gene prognostic signatures constructed for HCC.

Study	Signature	Genes	Formula of risk score	Statistical methods	AU 5y) tra
Our study	8-gene	hypoxia-related immune genes	0.017176×S100A10+0.226828×MAPT+ 0.021352× CACYBP+0.139515×BIRC5+0.064381×KITLG+0.043464×SPP1+0.145751×STC2+(-0.02423)×GHR	1) PPI network; 2) Univariate Cox; 3) Multivariate Cox; 4) LASSO Cox; 5) Correlation analysis	0.7 0.6 N=
Gu et al, 2021	5-gene	immune-related genes	0.307×LDHA+0.268×PPAT+0.455×BFSP1+0.234 ×NR0B1+ 0.109 ×PFKFB4	1) LASSO Cox	0.8 0.7 (T(
Pan et al, 2020	4-gene	immune-related genes	0.024×BIRC5+0.139 ×PLXNA3+0.213 × FGF13+0.144×GAL	1) TFs-regulatory network; 2) Univariate Cox; 3) Multivariate Cox; 4) LASSO Cox;	0.7 0.6 N=
Zhang et al, 2020	9-gene	immune-related genes	0.0250×HSPA4+0.0213×RBP2+0.2424×MAPT+ 0.1347×TRAF3+0.0057×NDRG1+0.0330×NRAS+0.1501×GAL+0.0799×IL17D+0.0001×SPP1	1) TFs network; 2) Univariate Cox; 3) Multivariate Cox; 4) LASSO Cox;	0.8 (T(
Xu et al, 2020	8-gene	immune-related genes	0.00109×CKLF+0.23932×IL12A+0.00067×CCL20 +0.01209×PRELID1+0.09808 ×FYN+0.08045×GLMN+0.07259×ACVR2A + 0.00434×CD7	1) Cox proportional hazards regression; 2) Univariate Cox; 3) Multivariate Cox; 4) LASSO Cox;	0.7 0.8 (T(N=

Figures

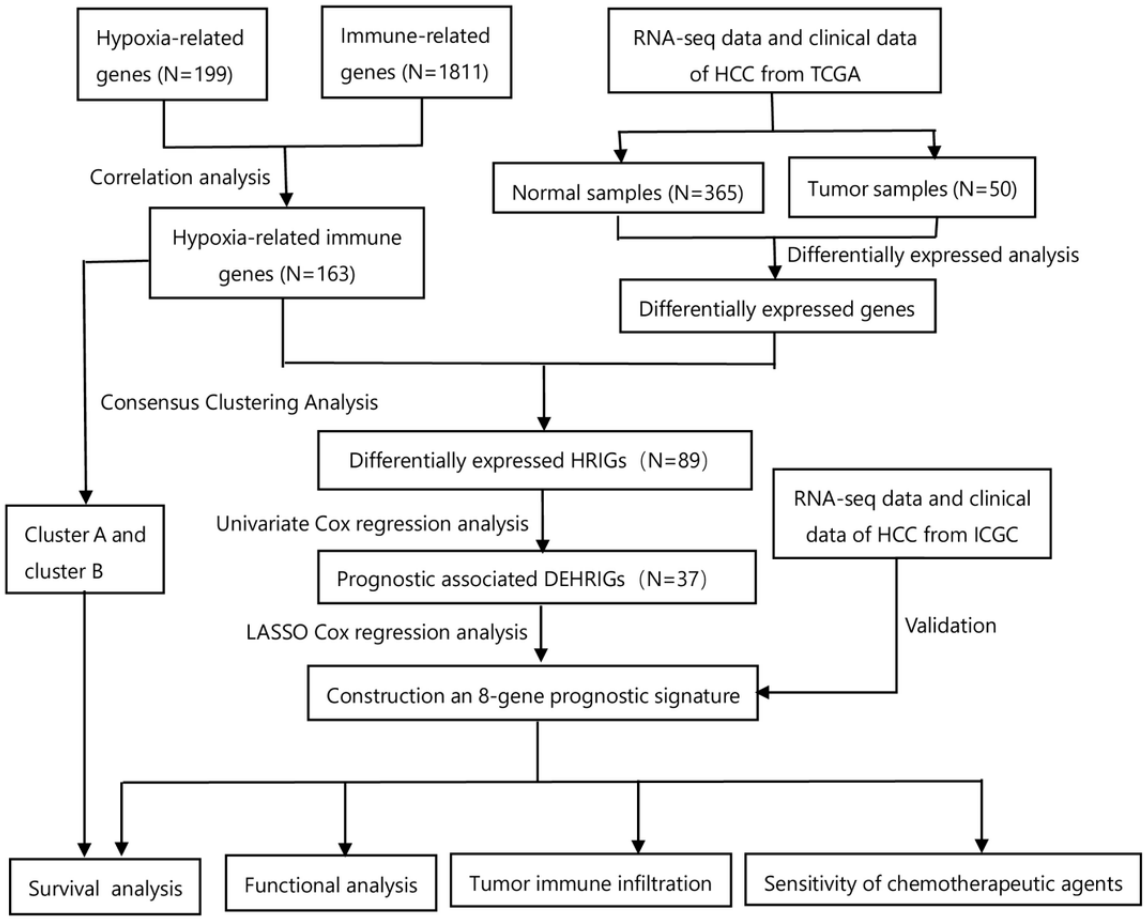

Figure 1

Flow diagram of the study.

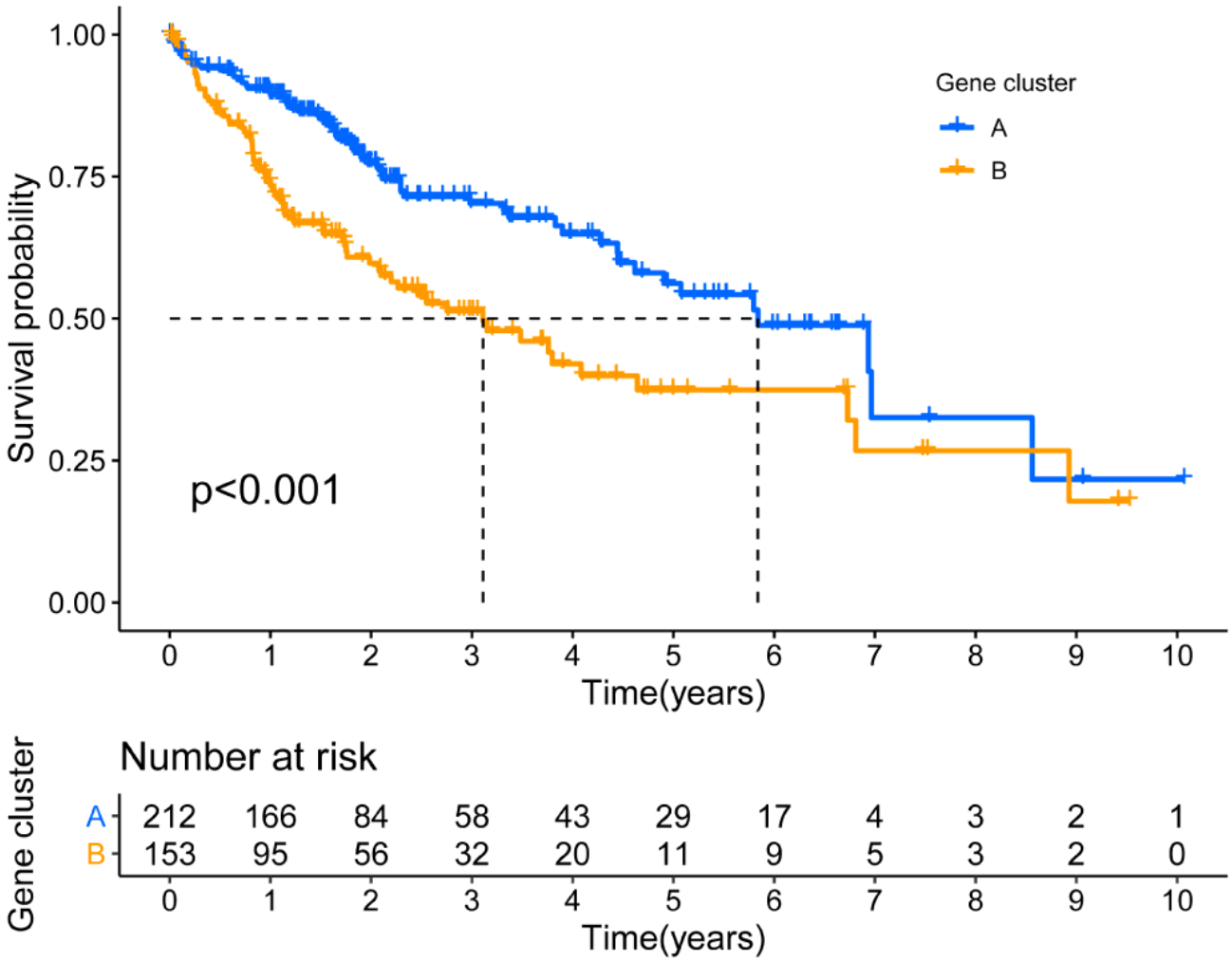

Figure 2

Kaplan–Meier survival curves of OS for patients with HCC in two clusters of the TCGA cohort.

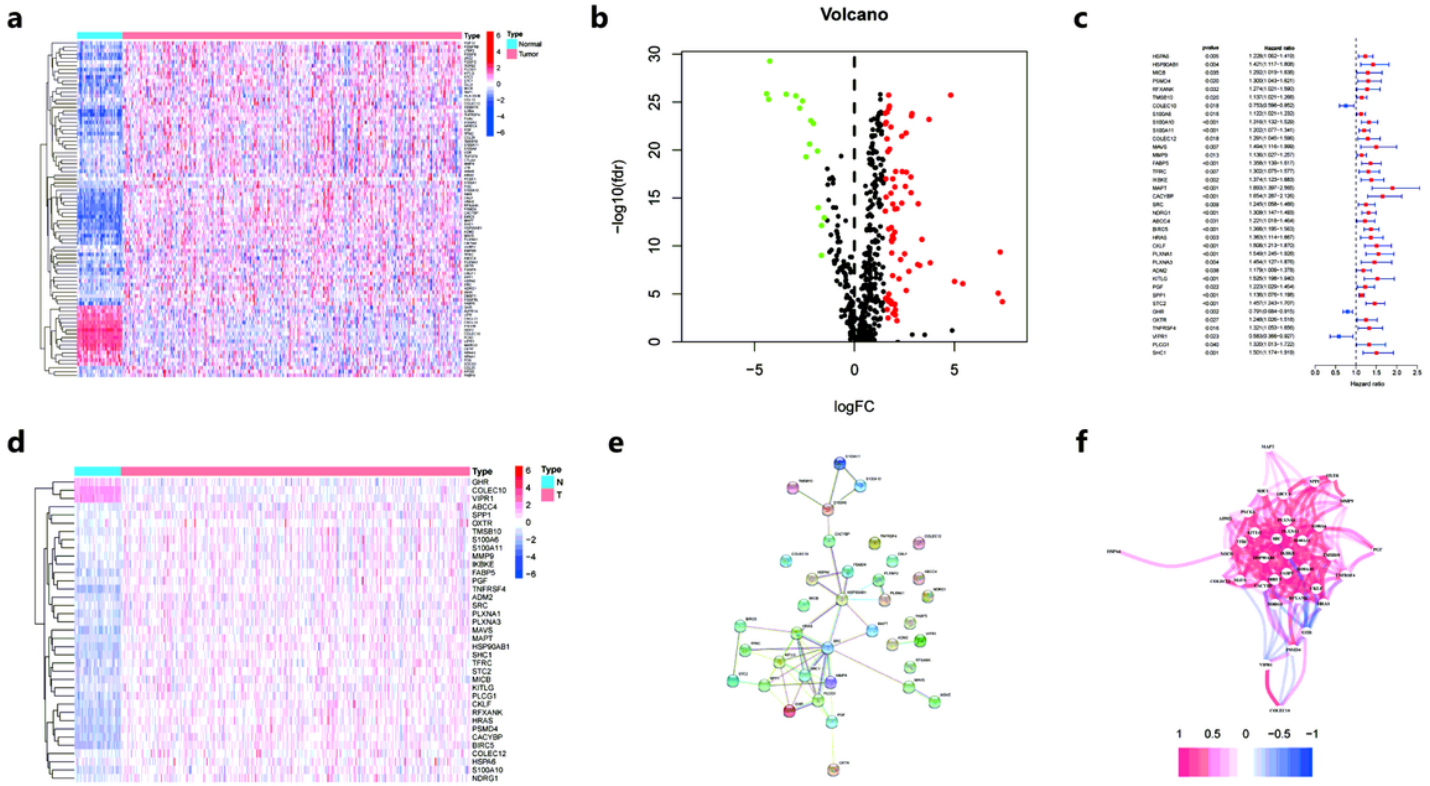

Figure 3

Identification of DEHRIGs associated with prognosis of patients with HCC in the TCGA cohort. a. Heatmaps for the DEHRIGs between HCC samples and paracancerous samples. b. Volcano plots for the DEHRIGs between HCC samples and paracancerous samples. c. Forest plots to identify the prognosis-related DEHRIGs. d. Heatmaps for the prognosis-related DEHRIGs. e. The PPI network of prognosis-related DEHRIGs. f. The correlation network of prognosis-related DEHRIGs.

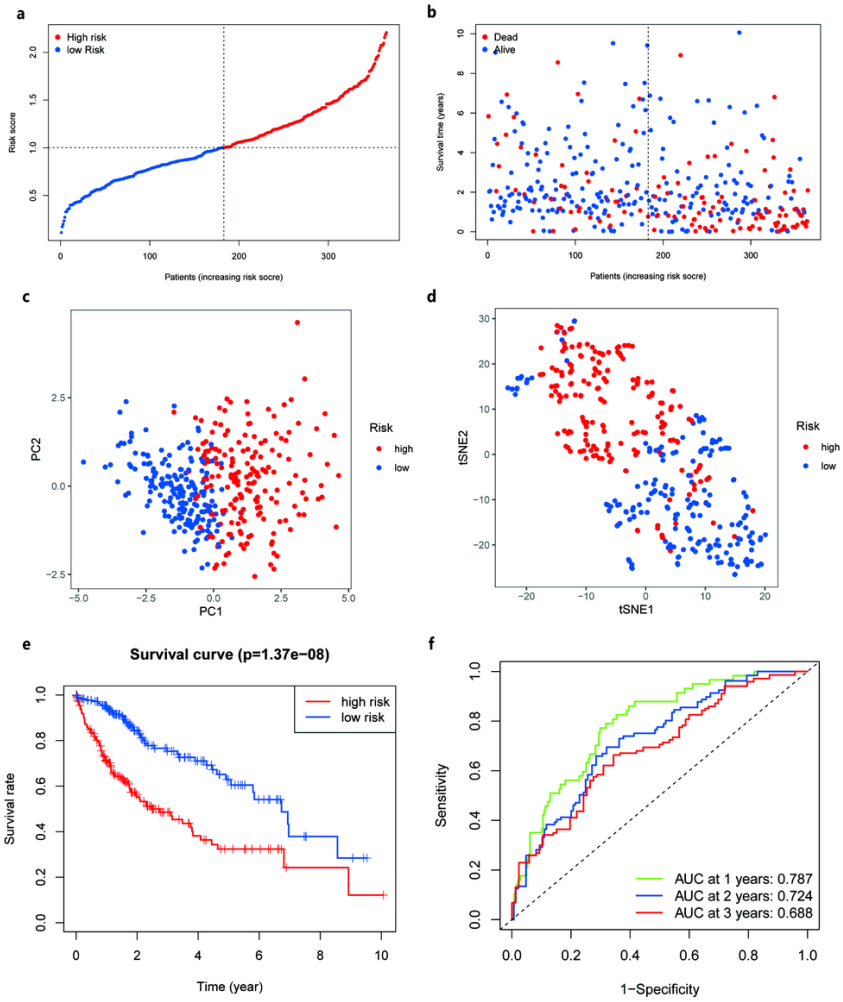

Figure 4

Construction and assessment of the HRIG prognostic signature in the TCGA cohort. a. The permutation of risk scores of patients with HCC and identified the median risk score. b. The scatter plot of survival time, survival state and risk score in the TCGA cohort. c. PCA plot showing the result of principal component analysis of the two groups (high-risk group and low-risk group) in the TCGA cohort. d. t-SNE analysis of the two groups (high-risk group and low-risk group) in the TCGA cohort. e. Kaplan-Meier survival curve of HRIG prognostic signature in the TCGA cohort. f. The AUCs for the risk score was calculated according to the ROC curve.

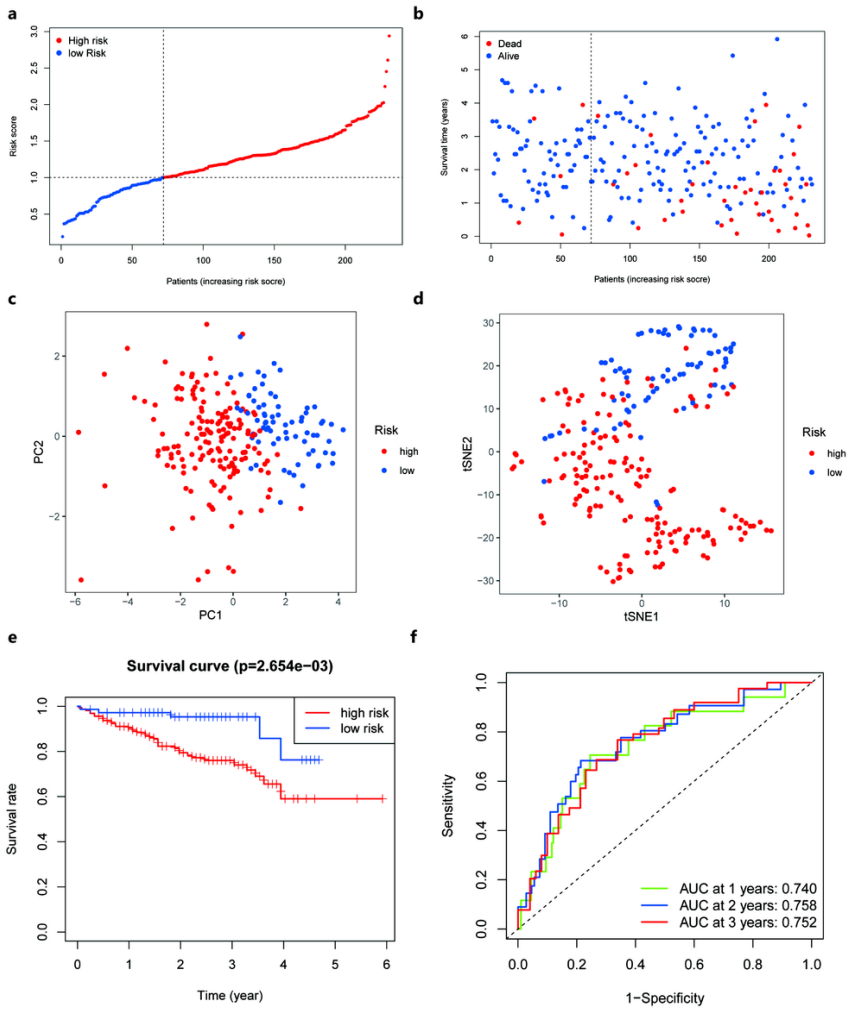

Figure 5

Validation of the HRIG prognostic signature in the ICGC cohort. a. The permutation of risk scores of patients with HCC and identified the median risk score. b. The scatter plot of survival time, survival state and risk score in the ICGC cohort. c. PCA plot showing the result of principal component analysis of the two groups (high-risk group and low-risk group) in the ICGC cohort. d. t-SNE analysis of the two groups (high-risk group and low-risk group) in the ICGC cohort. e. Kaplan-Meier survival curve of HRIG prognostic signature in the ICGC cohort. f. The AUCs for the risk score was calculated according to the ROC curve in the ICGC cohort.

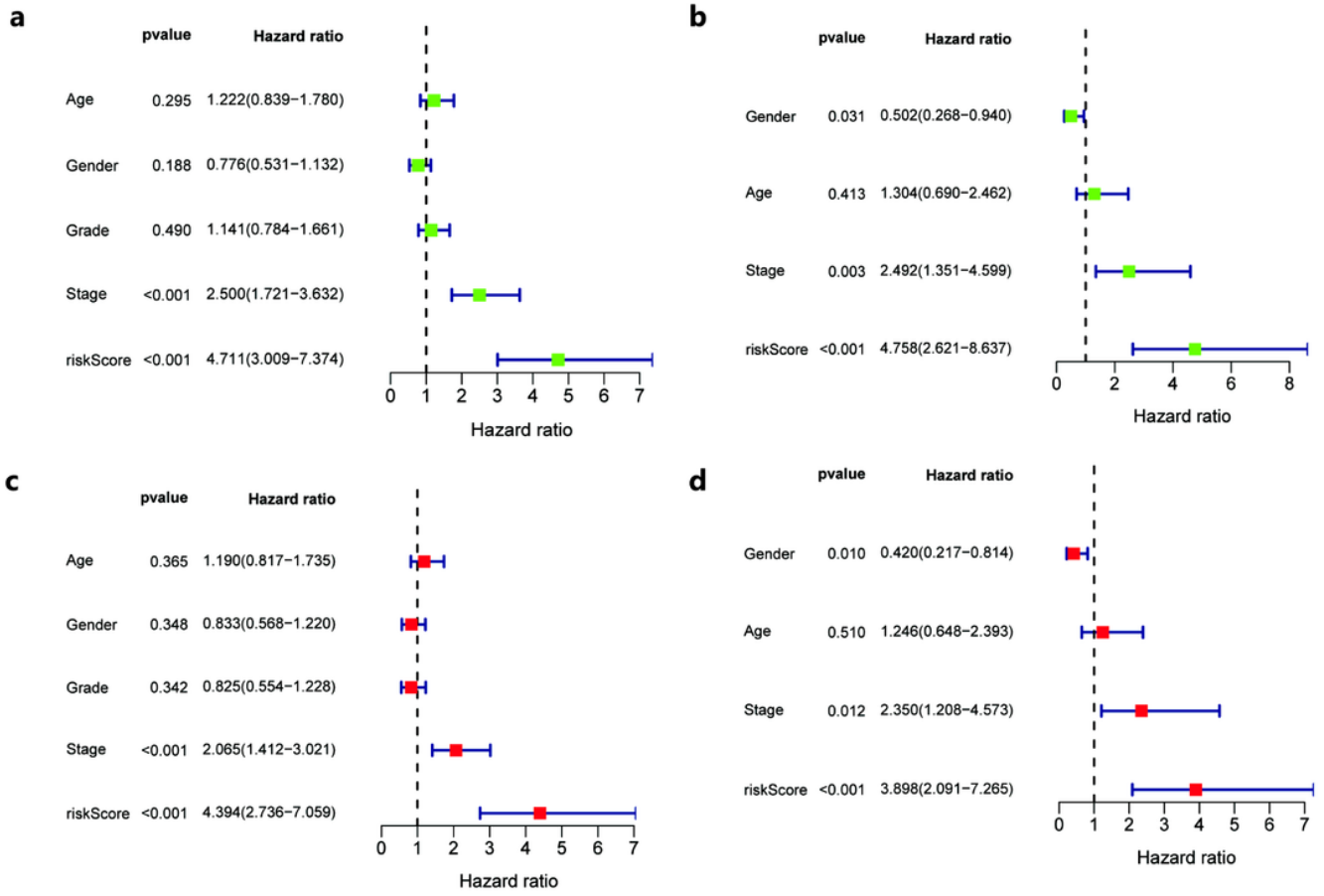

Figure 6

Cox regression analyses for identifying independent predictors of OS in the TCGA cohort and the ICGC cohort. Univariate Cox regression analyses in the TCGA cohort (a) and the ICGC cohort (b). Multivariate Cox regression analyses in the TCGA cohort (c) and the ICGC cohort (d).

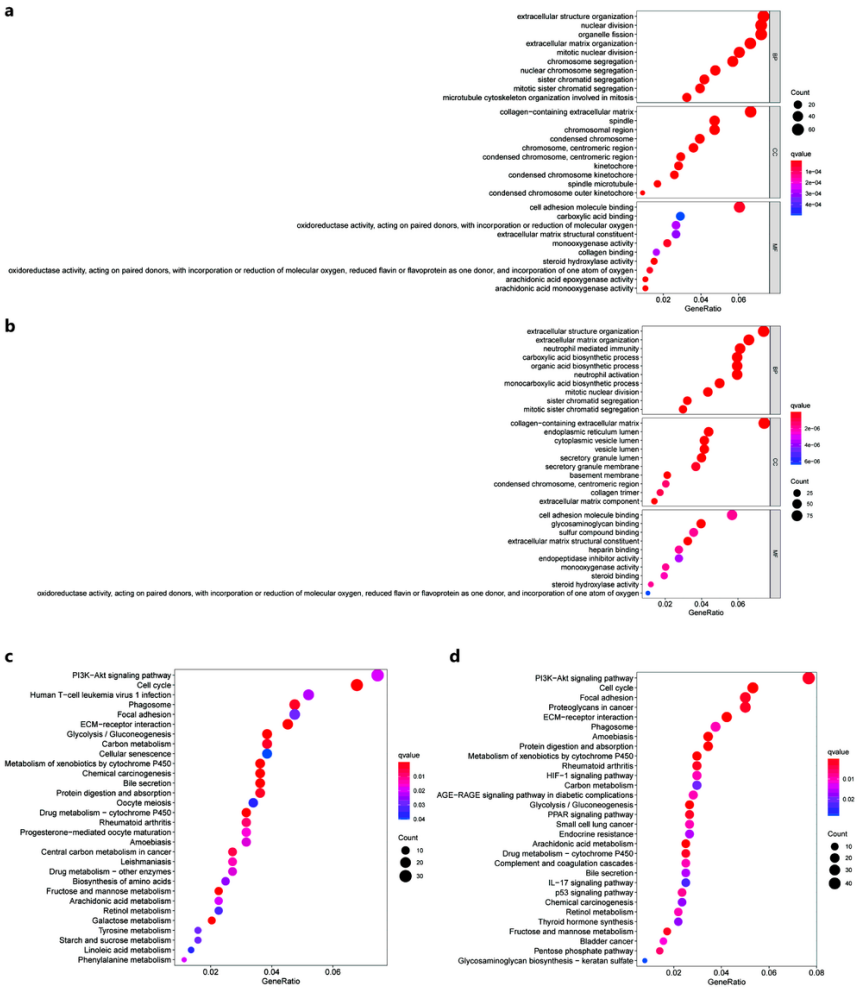

Figure 7

The results of GO and KEGG analyses. Biological processes related to DEGs between high-risk group and low-risk group in the TCGA cohort (a) and the ICGC cohort (b). Significantly enriched pathways related to DEGs between high-risk group and low-risk group in the TCGA cohort (c) and the ICGC cohort (d).

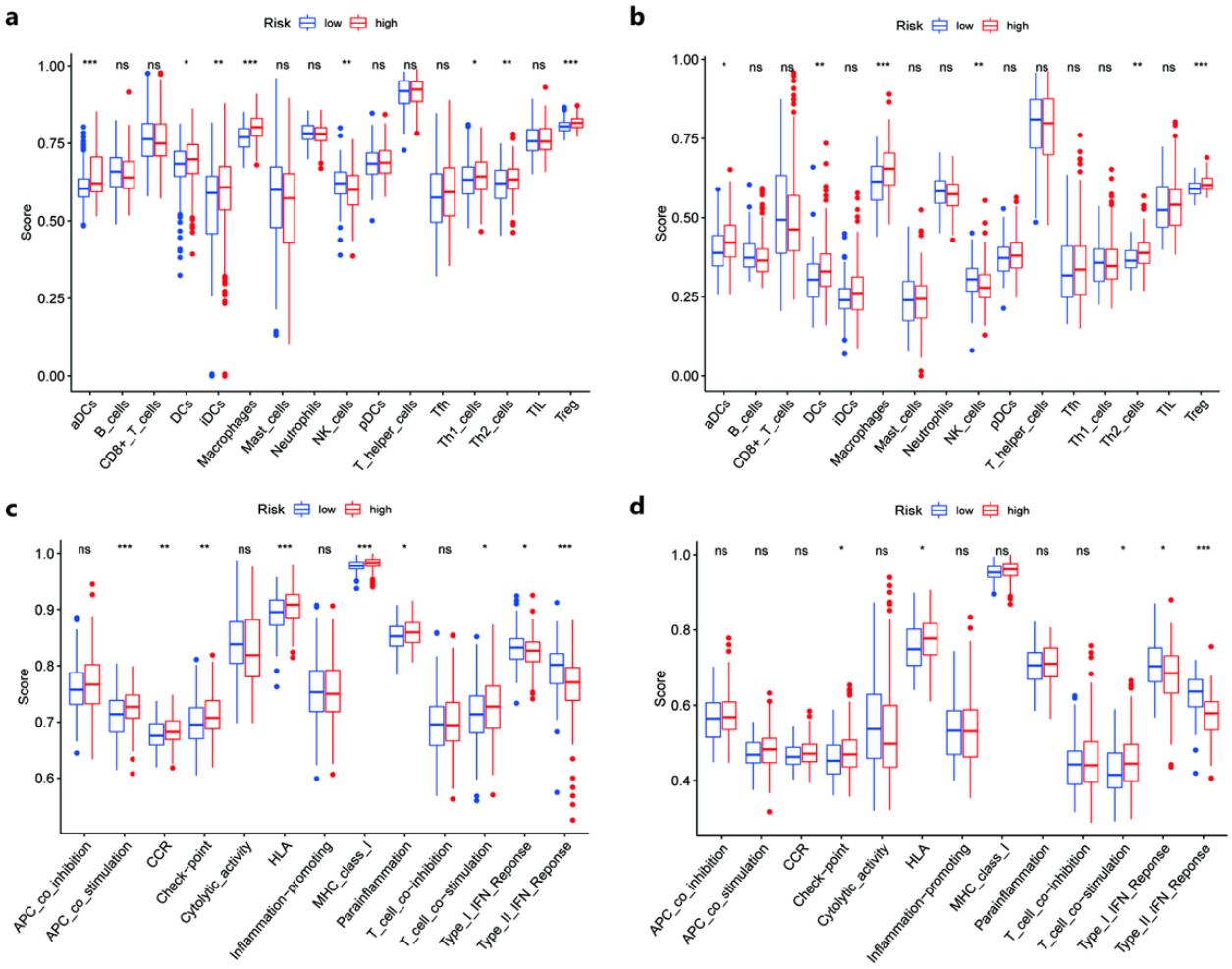

Figure 8

Evaluation of tumor immune infiltration in low- and high-risk groups. Comparison of the scores of immune infiltrating cells between low- and high-risk group in the TCGA cohort (a) and the ICGC cohort (b). Comparison of the scores of immune-related functions between low- and high-risk group in the TCGA cohort (c) and the ICGC cohort (d).

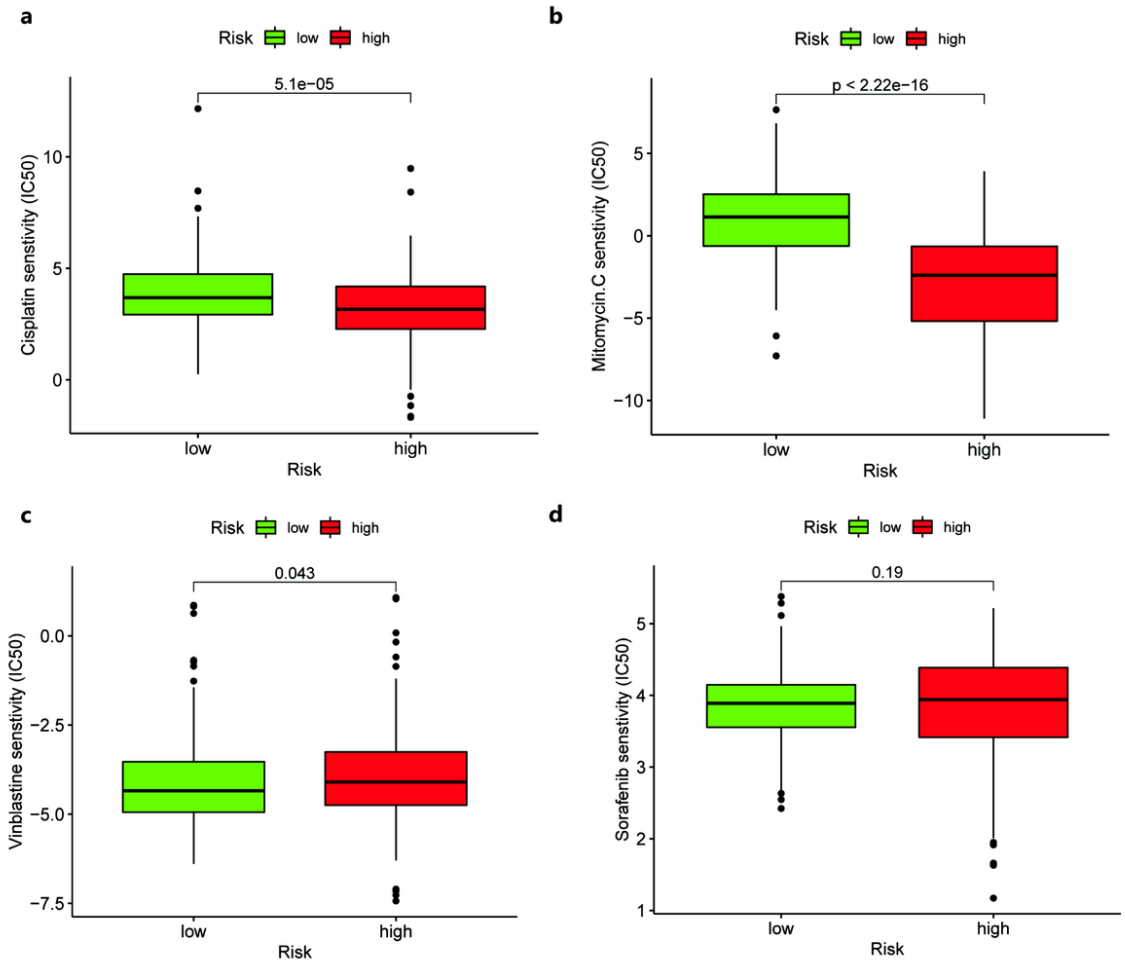

Figure 9

The correlation between the risk model and the efficacy of chemotherapeutic agents. a. Sensitivity analysis of cisplatin in patients at different risk. b. Sensitivity analysis of mitomycin.c in patients at different risk. c. Sensitivity analysis of vinblastine in patients at different risk. d. Sensitivity analysis of sorafenib in patients at different risk.

Supplementary Files

This is a list of supplementary files associated with this preprint. Click to download.

- Additionalfile1.docx
- Fig.S1.tif